CARBON 52 (2013) 65–73

Available at www.sciencedirect.com

SciVerse ScienceDirect

journal homepage: www.elsevier.com/locate/carbon

NMR a critical tool to study the production of carbon fiber from lignin

Marcus Foston [a], *Grady A. Nunnery* [b], *Xianzhi Meng* [a], *Qining Sun* [a], *Frederick S. Baker* [b], *Arthur Ragauskas* [a,*]

[a] *BioEnergy Science Center, School of Chemistry and Biochemistry, Institute of Paper Science and Technology, Georgia Institute of Technology, 500 10th St., Atlanta, GA 30332, United States*

[b] *Materials Science and Technology Division, Oak Ridge National Laboratory, Oak Ridge, TN 37831-6087, United States*

ARTICLE INFO

Article history:
Received 7 April 2012
Accepted 6 September 2012
Available online 14 September 2012

ABSTRACT

The structural changes occurring to hardwood Alcell™ lignin as a result of fiber devolatilization/extrusion, oxidative thermo-stabilization and carbonization are investigated in this study by solid-state and solution nuclear magnetic resonance (NMR) spectroscopy techniques. Solution based ^{1}H–^{13}C correlation NMR of the un-spun Alcell™ lignin powder and extruded lignin fiber detected modest changes occurring due to fiber devolatilization/extrusion in the type and proportion of aliphatic side-chain carbons or monolignol inter-unit linkages. Molecular weight analysis by gel permeation chromatography (GPC), along with an additional ^{31}P NMR method used to indicate changes in terminal hydroxyl functionality, suggest fiber devolatilization/extrusion causes both chain scission and condensation reactions. ^{1}H CRAMPS (combined rotation and multiple-pulse spectroscopy) and ^{13}C cross-polarization/magic angle spinning (CP/MAS) spectra of extruded and stabilized lignin fibers indicate stabilization severely reduces the proportion of methoxy groups present, while also increasing the relative proportion of carbonyl and carboxyl-related structures, typically associated with cross-linking chemistries. ^{13}C direct-polarization/magic angle spinning (DP/MAS) analysis of stabilized and carbonized fibers shows an increased relative amount of carbon–carbon bonds on aryl structures and a relative decrease of aryl ethers. DP/MAS dipolar dephasing experiments suggest that a majority of non-protonated carbons convert from carbonyl to aryl and condensed aryl structures during carbonization.

1. Introduction

Carbon fibers are characterized by properties such as high stiffness, high tensile strength, low density, elevated temperature tolerance, and low thermal expansion. These high performance properties make carbon fibers important engineering materials in advanced composites for a variety of industries, including aerospace, civil engineering, automotive and wind-power applications [1,2]. Many of these enhanced material characteristics can be attributed to the orientation of graphite layers, which are mostly aligned parallel to the long axis of the fiber. Typically, carbon fibers are produced by first spinning a polymer precursor commonly rayon, polyacrylonitrile (PAN) or petroleum pitch [3]. Polymer chain alignment is then enhanced using chemical and mechanical processes such as fiber drawing [4]. These precursor fibers are usually then subjected to an oxidative thermo-stabilization to prevent shrinking, melting and fiber fusing by cross-linking at the fiber surface [4,5]. Following stabilization, carbonization is achieved at high temperatures in an inert atmosphere to drive off non-carbon atoms and produce columnar graphene-like filaments [4,5].

* *Corresponding author:* Fax: +1 404 894 4778.
E-mail address: art.ragauskas@chemistry.gatech.edu (A. Ragauskas).
0008-6223/$ - see front matter
http://dx.doi.org/10.1016/j.carbon.2012.09.006

One of the most commonly studied precursor materials for carbon fiber commercial production is PAN [4]. However, PAN derived carbon fiber utilization is typically limited to high performance grade applications, not only due to its superior mechanical properties but also in part because of the high production cost associated with PAN synthesis, low yield and slow graphitization [4]. Within the last decade or so, a considerable amount of research has shown lignin is an appropriate precursor for carbon fibers [6–8]. Lignin is one of three major biopolymers in the cell wall of plants, along with cellulose and hemicellulose. Because of this, lignin is the second most abundant terrestrial material, typically comprising ~15–30% of the dry weight of woody plants and therefore is considered a very suitable, readily available, relatively inexpensive and a renewable carbon fiber precursor [9,10]. Lignin is described as a complex, racemic, cross-linked and highly heterogeneous aromatic macromolecule based on hydroxycinnamyl alcohol monomers with various degrees of methoxylation (*p*-coumaryl, coniferyl and sinapyl alcohol) [10].

Lignin is a co-product of (1) kraft or sulfite pulping processes for paper-making, (2) organosolv pulping treatments, and (3) carbohydrate enzymatic hydrolysis of pretreated biomass typically resulting from bioethanol production [7]. The utilization of this lignin, whose yearly worldwide production is estimated at ~25–30 million tons a year [11], is currently fairly limited to a fuel source for pulp/paper production in the recovery boiler and in formulations for dispersants, adhesives and surfactants [7]. In this study, we focus on carbon fiber generated from Alcell™ lignin, a co-product lignin resulting from a proprietary organosolv pulping treatment [12]. Alcell™ lignin has many features which distinguish it from kraft and sulfite lignin such as low molecular weight, altered solubility and glass transition temperature [12]. Though currently substantial amounts of biomass are processed annually, mainly for pulp production, to achieve the large-scale production of fuels, chemicals, and materials from renewable biomass resources significant product diversity and value-added co-utilization of the complete plant cell wall will be vital [7,13,14]. Therefore, research such as this, which is focused on gaining a detailed understanding of the mechanisms involved in the conversion of lignin to a highly value-added product, i.e. carbon fiber, is important to the continued development of biomass based production of renewable fuels and materials [14].

Techniques such as Fourier transform infrared (FTIR) [6,15–17] and X-ray photoelecton (XPS) [6,18] spectroscopy have been commonly used to analyze carbon fiber production from a variety of feedstocks. For example, Shin et al. utilized FTIR to investigate the changes in carbon fiber generated from petroleum pitch on fiber surface functionalities. They determined as carbonization temperature increased, the amount of oxygen-containing functional groups was reduced. This caused the fibers to become more hydrophobic, an important observation with respect to carbon fiber/polymer composite formation [19]. Whereas, another group of researchers found using both FTIR and XPS techniques, increased levels of carbonyl and carboxyl structures in lignin fibers after oxidative thermo-stabilization, subsequently relating this to cross-linking at the fiber surface [6]. However, FTIR and XPS do not provide the chemical specificity of NMR, only resolving chemical bonding information rather than the specific presence of functionalities, linkages and chemical environments. NMR, especially solid-state techniques, is a tool particularly well-suited to study both lignin and carbon fiber because of their limited solubilities and inherent chemical and structural complexity. This information can be used to improve processing conditions and understand how the resulting structures in the carbon fiber may enhance the mechanical properties of lignin-based composites.

2. Experimental

2.1. Materials

Alcell™ lignin from hardwood sources was supplied by Lignol Innovations, Ltd. of Vancouver, Canada. Deuterated solvents (99 at.% D) were purchased and used as received from Cambridge Isotopes. All other solvents and reagents were obtained from Sigma–Aldrich.

2.2. Carbon fiber production

Melt spinning of the Alcell™ lignin fiber precursor was accomplished using a single filament Dynisco Laboratory Mixing Extruder (LME) with winding unit. Multifilament spinning trials were conducted using a pilot scale melt spinning unit, 4-zone custom-built melt spinning extruder (5/8 inch) (Alex James and Associates; Greenville, SC) adapted with a Koch static mixer, a spin head housing a Zenith metering pump, a 12-hole spinneret, with each hole being 150 μm in diameter. The unit consists of a hopper, single-screw extruder with four heating zones, a Koch static mixer, a spin head housing a Zenith metering pump, and a spinneret assembly. Before fiber melt spinning, dried lignin was pelletized using a continuous 4-zone single-screw Randcastle compounding extruder (5/8 inch) adapted with a 2-hole strand die, each hole being 3 mm in diameter. The zone temperatures of the pelletizer varied between 130 and 150 °C. After suitable melt spinning conditions were established (zones 1–4, ranging from 135 to 153 °C), fibers were wound onto a winder at 400 m per min. The approximate residence time in this extruder was ~25 min. After suitable melt spinning conditions were established, the take-up (winding) speed was varied to change the drawdown ratio and therefore obtain fibers of various diameters, including the target diameter of 10 μm for carbon fiber production [20].

Heat treatment studies to determine the appropriate oxidative-stabilization conditions for lignin fibers were conducted using a Lindberg Blue M 4L Box Furnace, modified for increased air flow and distribution, using an air flow rate of 20 L/min and slow heating to render the fibers infusible. Carbonization studies at temperatures ranging from 400 to 1000 °C were carried out on a Lindberg Blue M 2.54-cm diameter tube furnace with a nitrogen flow rate of 1 L/min after purging at 10 L/min for 15 min [20]. Further details on both the oxidative-stabilization and carbonization process are restricted due to export controls.

2.3. Characterization

2.3.1. Solid state NMR

The carbon fiber sample after oxidative thermo-stabilization and carbonization were prepared for solid NMR by pulverizing the fibers via vibrational ball-milling at 25 Hz for 15 min at room temperature. ^{13}C solid NMR samples were mixed with an equal weight of hydrated magnesium silicate to effectively reduce macro-current generation under radio frequency excitation and facilitate probe tuning. Lignin precursor and extruded fiber samples were prepared in a more typical fashion without the addition of hydrated magnesium silicate. All samples were added into 4-mm cylindrical ceramic MAS rotors. Solid-state NMR measurements were carried out on a Bruker Avance-400 spectrometer operating at frequencies of 100.55 MHz for ^{13}C and 399.875 MHz for ^{1}H NMR in a Bruker double-resonance MAS probehead at spinning speeds of 12 kHz for all experiments. ^{13}C CP/MAS experiments utilized a 5 μs (90°) ^{1}H pulse, 2.0 ms contact pulse, 4 s recycle delay and 8 K scans. ^{13}C DP/MAS experiments utilized a 6 μs (90°) ^{13}C pulse, 6 s recycle delay and 8 K scans. The dipolar dephasing sequence gates the decoupler off for 50 μs, as a simple spectral-editing method for generating a sub-spectrum of non-protonated carbons and mobile groups, such as rotating methyl groups. Baseline corrected spectra were processed with 75 Hz exponential line broadening. ^{1}H CRAMPS experiments used a W-PMLG multiple pulse sequence with a 2.5 μs (90°) ^{1}H pulse, 128 scans and 4 s recycle delay. Recycle delays for ^{1}H and ^{13}C CP experiments were determined by a series experiments with increasing recycle delays to ensure that all sites were >90–95% relaxed.

2.3.2. Heteronuclear Single Quantum Coherence NMR

Heteronuclear Single Quantum Coherence (HSQC) experiments were carried out at 55 °C in a Bruker Avance-400 spectrometer equipped with z-gradient double resonance broad band observation probe using a gradient enhanced sequence. The spectral widths were 11.0 and 180.0 ppm for the ^{1}H and ^{13}C dimensions, respectively. The HSQC analysis was performed using a standard Bruker pulse sequence with a 5 μs 90° pulse, 0.11 s acquisition time, a 1.5 s recycle delay, a $^{1}J_{C-H}$ of 145 Hz, acquisition of 128 complex data points and 128 scans. NMR samples were prepared as follows: 60 mg dried lignin fiber sample was added to 0.60 g of DMSO-d_6 and stirred at 55 °C for 1 h after dry N_2 purge. The resulting solution was transferred directly into a 5 mm NMR tube after dry N_2 purge [21].

2.3.3. ^{31}P NMR spectral analysis

All ^{31}P NMR lignin spectra were acquired in 3:2 volume ratio of pyridine:$CDCl_3$ with 0.469 mol/L of cyclohexanol as a internal standard (145 ppm) using a Bruker Avance-400 MHz spectrometer at 25 °C [22]. Lignin samples (0.020 g) were dissolved in 0.50 mL of the above solvent system and *in situ* derivatization of the lignin samples directly in the NMR tube was achieved with 0.1 mL of 2-chloro-4,4,5,5-tetramethyl-1,3,2-dioxaphospholane (TMDP). The operational frequency for the ^{31}P nucleus was 161.95 MHz, an inverse gated decoupling sequence was used with a 21 s recycle delay and 128 scans were collected.

2.3.4. Gel permeation chromatography

Acetylation of lignin was carried out according to the published procedure [23]. Dry lignin (20 mg) was dissolved a 1:1 mixture of acetic anhydride/pyridine mixture (1.00 mL) and stirred at 25 °C overnight. The reaction mixture was quenched with ethanol (2.0 mL) and then mixed with 2.0 mL of tetrahydrofuran (THF), filtered through a 0.45 μm filter and placed in a 2 mL auto-sampler vial. The molecular weight distributions of the acetylated lignin samples were then analyzed on an Agilent GPC SECurity 1200 system equipped with four Waters Styragel columns (HR1, HR2, HR4, HR6), Agilent refractive index (RI) detector and Agilent UV detector (270 nm) using THF as the mobile phase (1.0 mL/min) with injection volumes of 20 μL. A calibration curve was constructed based on eight narrow polystyrene standards ranging in molecular weight from 1.5×10^3 to 3.6×10^6 g/mol. Data collection and processing were performed using Polymer Standards Service WinGPC Unity software (Build 6807). Molecular weights (M_n and M_w) were calculated by the software relative to the polystyrene calibration curve. Polydispersity index (PDI) was calculated by dividing M_w by M_n.

3. Results and discussion

The structural changes occurring to hardwood Alcell™ lignin as a result of fiber devolatilization/extrusion were first investigated in this study by a solution NMR technique, ^{1}H–^{13}C Heteronuclear Single Quantum Coherence (HSQC) experiment, in an effort to gain details on chemical functionality. We also attempted to analyze fibers after oxidative thermo-stabilization and carbonization but as expected, these samples displayed at best partial solubility, hence precluding this analysis on these samples. By the strong appearance of the α-carbon C–H correlation (see Fig. 1) and its relative volume integration (integration of A_α over total integration of all peaks), β-aryl ether linkages (A) were found to be one of the major lignin inter-unit linkage in both the un-spun Alcell™ lignin powder and extruded lignin fiber; however, significant traces of phenyl coumaran (B) and resinol (C) were also detected via C_α–H correlations at δ_c/δ_H 87.5/5.4 (B_α), and 85.7/4.6 (C_α) ppm [24,25], respectively (structures shown in Fig. 2). Another dominant C–H lignin resonance due to methoxyl groups was observed at δ_c/δ_H 55.7/3.8 ppm. The presence of aromatic lignin units syringyl (S) and guaiacyl (G) units (structures shown in Fig. 2) was confirmed by the overlapping contours for $S_{2,6}$, G_2, and G_6 at δ_c/δ_H 104.3/6.7 ($S_{2,6}$), 111.1/6.9 (G_2), and 119.8/6.7 (G_6), [24,25] respectively.

Based on spectral integrations for the two samples, the relative proportion of syringyl to guaiacyl (S:G) units does not significantly change, displaying a slight reduction from ~1.4 to 1.0 upon devolatilization/extrusion. This may suggest demethoxylation is occuring, however; for reasons explored by Zhang and Gellerstedt ^{1}H–^{13}C HSQC experiments are at best semi-quantitative when conducted on complex polymer systems such as lignin [26] and is therefore difficult to interpret with respect to the statistical significant of change. Comparison of the total integrated areas of A_α, B_α, and C_α aliphatic carbons to methoxyl group carbon suggests the relative amount of aliphatic side-chain carbons or inter-unit linkages

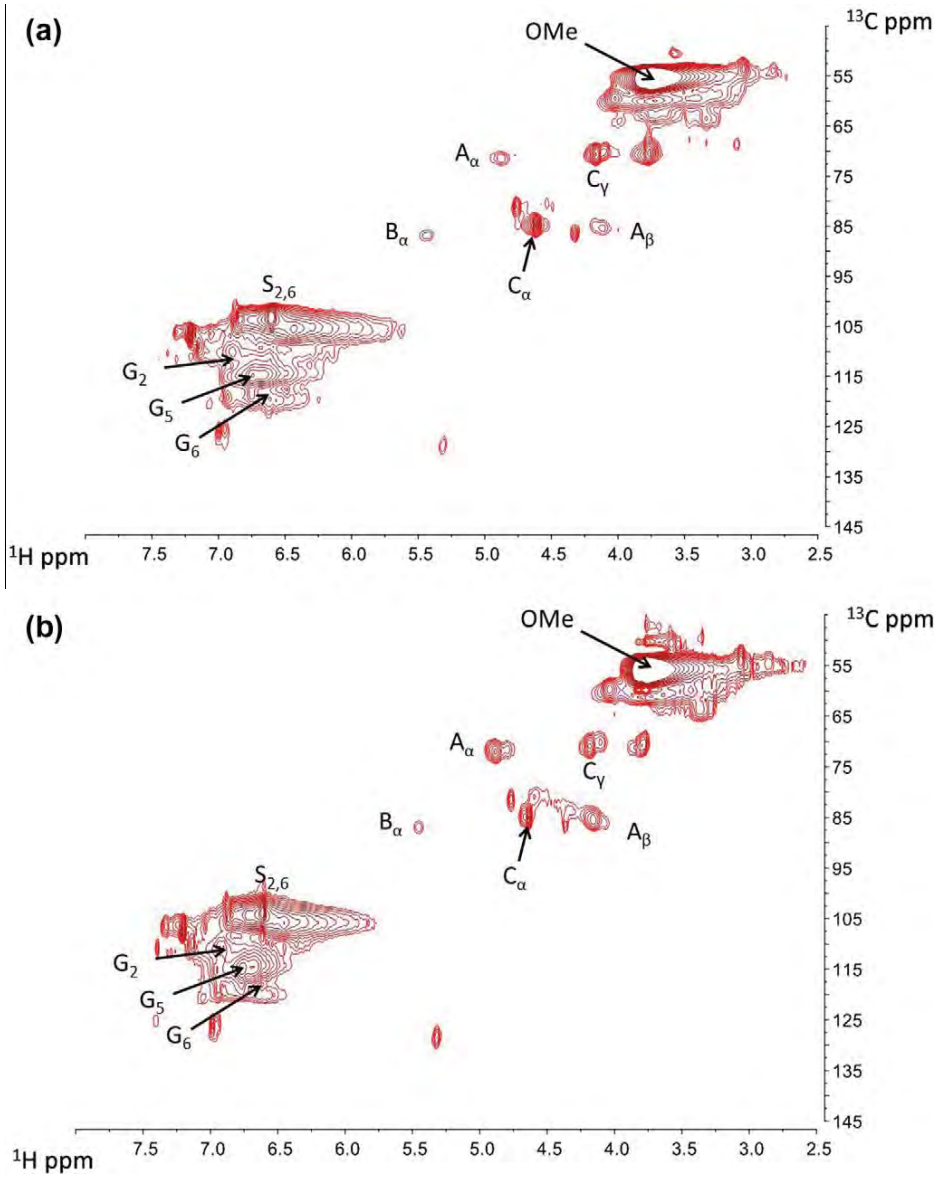

Fig. 1 – 2D ^{13}C–^{1}H heteronuclear single quantum correlation (HSQC) NMR spectra of Alcell™ lignin samples in DMSO-d_6 at 55 °C. (a) Un-spun Alcell™ lignin powder and (b) extruded Alcell™ lignin fibers after devolatilization and extrusion; A: β-aryl ether linkage; B: phenylcoumaran; C: resinol; S: syringyl; G: guaiacyl.

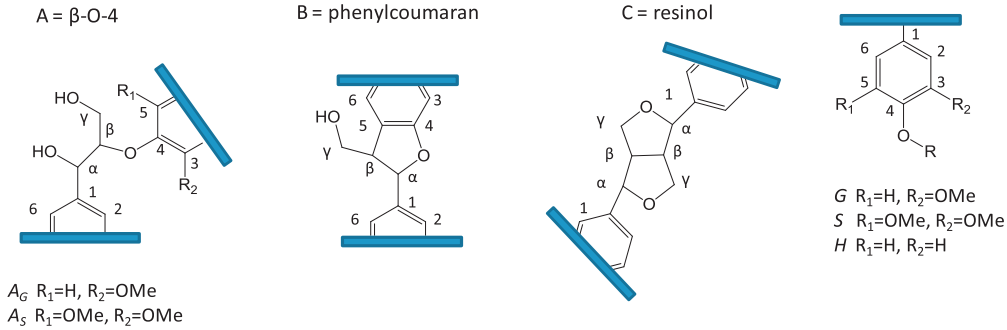

Fig. 2 – Common chemical moieties in lignin.

decreases with devolatilization/extrusion displaying significant relative decreases particularly with β-aryl ether and resinol linkages. However, the total integrated areas of S_2 and G_2 aromatic carbons to methoxyl group carbon suggest devolatilization/extrusion does little to change the relative proportion of total aromatic monomer units with respect to methoxy content. These observations may be significant to fiber processing and eventual fiber properties because they suggest either chain scission and/or condensation reactions are occurring.

A valuable tool for estimating the amounts and distribution of various hydroxyl and phenolic groups relies on ^{13}P NMR analysis of lignin derivatized *in situ* by 2-chloro-4,4,5,5-tetramethyl-1,3,2-dioxaphospholane (TMDP) [22]. In this method, the hydroxy functionality is analyzed following literature methods [27] and is summarized in Fig. 3 and Table 1. Though not fully descriptive of the entire lignin macromolecule, the results are indicative of the major lignin chemical structural characteristics and can be particularly useful when analyzing chain scission and condensation reactions. The results suggest that upon devolatilization/extrusion, a modest decrease in terminal aliphatic hydroxyl content occurs, which supports the above result with respect to decreasing of aliphatic side-chain carbons or inter-unit linkages. However, the amounts of terminal C-5 condensed phenolic structures increases with devolatilization/extrusion as seen at the chemical shift range of ~144–142 ppm. The ^{31}P NMR results seem to clarify the above HSQC observations on the relative proportion of S to G aromatic monomer units, showing the aromatic monomer ratio does not change significantly while also displaying reduction in carboxylic acid functionality.

In an effort to further investigate the structural changes occurring during devolatilization/extrusion, un-spun Alcell™ lignin powder and lignin fibers after devolatilization and extrusion were analyzed by gel permeation chromatography (GPC), and the resulting chromatographs are shown in Fig. 4. A common solvent used for GPC is tetrahydrofuran (THF) [28]; however, lignin displays a minimal solubility in that particular solvent. Therefore, these samples were acetylated using acetic anhydride/pyridine following a literature procedure [23], and the resulting molecular weights and polydispersities as determined by a polystyrene based relative calibration curve are summarized in Table 2. Both Fig. 4 and Table 2 indicate a near symmetric broadening in the lignin molecular weight distribution with a relatively un-shifted distribution center upon devolatilization and extrusion, which suggests that chain scission, due most likely to cleavage of aliphatic side-chains, and condensation reactions are indeed occurring as indicated above by ^{13}C and ^{31}P NMR. These types of changes in lignin monomer linkages and degree of polymerization seem to be linked to the adjustable time and temperature profile of devolatilization/extrusion, slightly altering lignin chemistry but more significantly chain flexibility, conformation and intramolecular bonding presumably further influencing fiber processing and properties. For example, Uraki et al. attributed the high spinnability of organosolv lignin obtained from birch wood by aqueous acetic acid pulping in part to the relatively large molecular weight polydispersity [29].

^{1}H CRAMPS (combined rotation and multiple-pulse spectroscopy) is a technique to obtain high-resolution solid-state ^{1}H NMR spectra [30]. Fig. 5 shows the ^{1}H CRAMPS NMR spectra of extruded and stabilized lignin fibers. The spectrum of the extruded sample has significant signal between 8.5 and 1.0 ppm. The spectra seem to include three major overlapping resonances at ~5.2, 4.1, and 3.3 ppm (a carrier frequency peak artifact is at ~6.0 ppm), attributed to α-aliphatic, β- and γ-aliphatic/methoxy and methoxy protons, respectively (see Table 3) [31,32]. Upon oxidative stabilization the downfield peak centered at ~5.2 ppm shifts to ~4.8 ppm, and the peak at 4.1 ppm disappears. This would indicate degradation or at least the conversion of the typical forms of lignin inter-unit linkages or aliphatic side-chain functionality upon stabilization. The

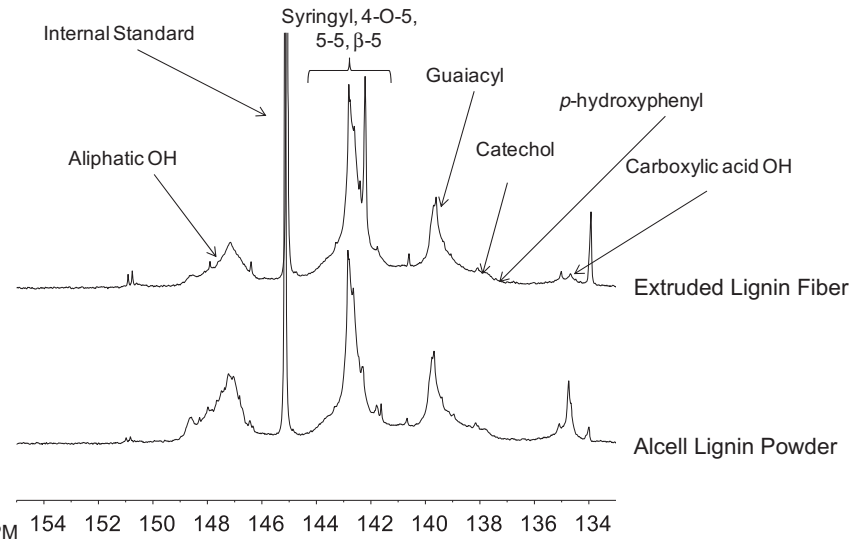

Fig. 3 – ^{31}P NMR spectra of un-spun Alcell™ lignin powder and Alcell™ lignin fiber after devolatilization and extrusion as a result of derivatization by TMDP.

Table 1 – Distribution of terminal hydroxyl and phenolic groups in un-spun Alcell™ lignin powder and Alcell™ lignin fibers after devolatilization and extrusion from ^{31}P NMR (mmol of OH/g of lignin).

	Aliphatic OH	Condensed and S units	G units	Catechol and H units	Carboxylic OH
Un-spun Alcell™ lignin powder	1.293	0.037	0.010	0.005	0.040
Extruded Alcell™ lignin fiber	0.853	0.047	0.012	0.005	0.015

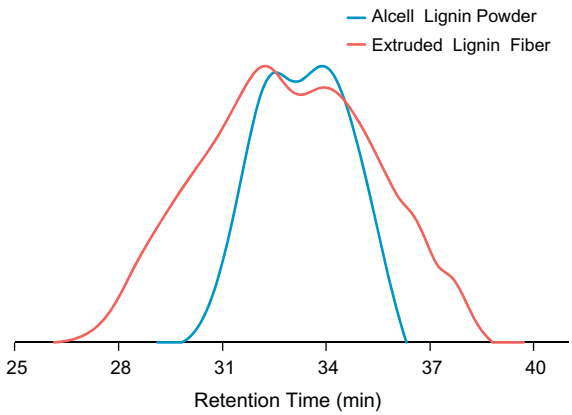

Fig. 4 – Gel permeation chromatography (GPC) in tetrahydrofuran of un-spun Alcell™ lignin powder and Alcell™ lignin fibers after devolatilization and extrusion derivatized with acetic anhydride.

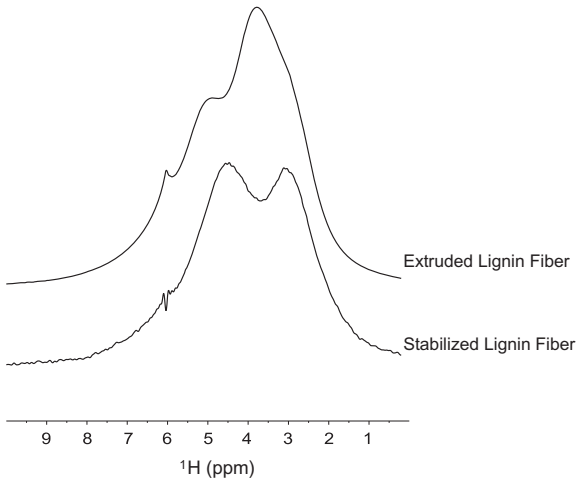

Fig. 5 – ^{1}H CRAMPS spectra of lignin fiber with a MAS condition of 12 kHz.

relative peak areas of the remaining aliphatic and methoxy protons change, actually displaying a slight population inversion. This spectral change indicate stabilization reduces the relative proportion of methoxy groups present, typically associated with the 3- and 5-carbon positions on the monolignol unit. Braun et al. have shown that demethoxylation is the major reaction occurring in the oxidization of kraft lignin, which drastically increases with heating to higher temperatures [6]. Unfortunately, the conducting nature of the carbon fiber samples made acquiring ^{1}H CRAMPS spectra of the carbonized fibers impossible.

The detailed information extracted from ^{1}H CRAMPS experiments can be limited because the broad overlapping appearance of solid state resonances and the resolution limit of such experiments [30]. In an effort to observe more spectral features and extract a higher detail of information, we also conducted ^{13}C cross-polarization and direct-polarization experiments. In comparison to ^{1}H, ^{13}C is a fairly insensitive and dilute nucleus [30]. Direct-polarization (DP) experiments directly excite and observe the carbon nuclei; however, the relaxation times for carbon in solid samples can be long. Therefore, DP experiments can be fairly long, and obtaining a truly quantitative spectrum difficult [30]. Cross-polarization (CP) experiments, on the other hand, excite protons, transfer that magnetization to carbon and then observe the carbon nuclei [30]. These experiments have much shorter recycle times; however, they require a long and high power spin-locking pulse. Again the conducting nature of the carbon fiber samples made acquiring ^{13}C CP spectra of the carbonized fibers problematic, which can be mitigated by intimate blending with an insulating powder containing no carbon, i.e. magnesium silicate.

Fig. 6 displays the ^{13}C CP/MAS NMR spectra of Alcell™ lignin powder, extruded and stabilized lignin fibers. The spectrum of the extruded sample is very similar to typical CP spectra of lignin and observed Alcell™ lignin spectrum, displaying a population of carbonyl groups and aryl ether, condensed aryl, aryl, aliphatic side-chain (C_α, C_β, and C_γ), methoxy, and aliphatic carbons at ~172, 141–152, 123–140, 110–123, 83–61, 55, and 30 ppm respectively (see Table 4) [33–35].

Upon oxidative stabilization, the relative proportion of aryl ether structures (involving β-O-4 linkages and methoxylated aromatic carbons) significantly decreases with respect to aryl and condensed aryl structures, going from a ratio of 0.57 to 0.29 (Aryl C-OR:Aryl C-R). Also, the resonances at ~83–61 ppm

Table 2 – GPC results of acetylated Alcell™ lignin samples.

	M_n (g/mol)	M_w (g/mol)	Polydispersity
Un-spun Alcell™ lignin powder	1.43×10^3	2.31×10^3	1.6
Extruded Alcell™ lignin fiber	1.09×10^3	5.70×10^3	5.2

Table 3 – Signal assignments for ^{1}H NMR of lignin [31,32].

Chemical Shift (ppm)	Assignments
11.0–14.0	Carboxylic acid
9.4–11.0	Aldehyde
8.5–9.4	Unsubstituted phenolic
7.9–8.5	Substituted phenolic
6.3–7.9	Aromatic and vinylic
4.0–6.3	Aliphatic (H_α and H_β)
3.5–4.0	Methoxy and H_γ

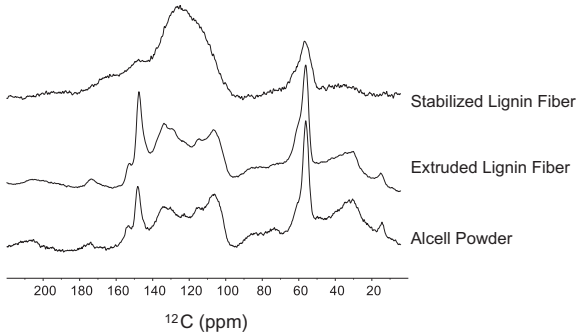

Fig. 6 – ^{13}C CP/MAS spectra of lignin and carbon fiber with a MAS condition of 12 kHz.

Table 4 – Signal assignments for CP/MAS and DP/MAS ^{13}C NMR of lignin [33–35].

Chemical Shift (ppm)	Assignments
>172	C-OOR
141–152	Aryl C-OR
123–140	Aryl C-R
110–123	Aryl C-H
~83	C_β
~75	C_α
~61	C_γ
55	$-OCH_3$
30	Aliphatic

attributed to side-chain inter-unit (C_α, C_β, and C_γ) carbons [34] almost completely disappear. The decreased intensity of the peak centered at 55 ppm again indicates that demethoxylation is a major reaction occurring in lignin fiber oxidative stabilization. The extruded lignin fiber spectrum shows the presence of carboxylic acid-type structures in the range of 180–170 ppm. The relative intensity of resonances assigned to these carbonyl and carboxylic acid structures seemingly persists or even slightly increases from ~2.2 to 4.2% of total carbon as a result of stabilization. Moreover, the relative intensity of the region from 170 to 160 ppm typically associated with esters and anhydrides also increases from below 1% to ~5.2% of total carbon with stabilization, which is significant because the presence of these functional groups is commonly attributed to cross-linking. These results are supportive of conclusions made in an earlier study by Braun et al. on the structural changes occurring during oxidative thermo-stabilization on lignin-based carbon fibers [6].

Fig 7 shows the DP NMR spectra of extruded, oxidative thermo-stabilized and carbonized Alcell™ lignin samples. The extruded and stabilized fiber DP spectra are very similar to that of the CP spectra seen above in Fig. 6, though as expected, in both cases the DP spectra seems to be more sensitive to the presence of carbonyl carbons than the CP spectrum. The DP spectra even more clearly demonstrate there is an increase in the proportion of carbonyl and carboxylic acid structures upon fiber oxidation. As the fiber is carbonized, the remaining methoxy content is reduced, the relative amount of carbonyl carbons decreases, and the relative proportion of aryl and condensed aryl carbons increases. These structural changes are a result of fiber pyrolysis, which drives off non-carbon atoms mainly in form of H_2O, CO, CH_4 and CO_2. These observations seem to trend with increasing carbonization temperature until the top spectrum in Fig. 7 is obtained. This spectrum represents the fiber carbonized at 1000 °C, displaying a single broad resonance from ~100–170 ppm, centered near 123 ppm, again representing mainly the presence of aryl and condensed aryl

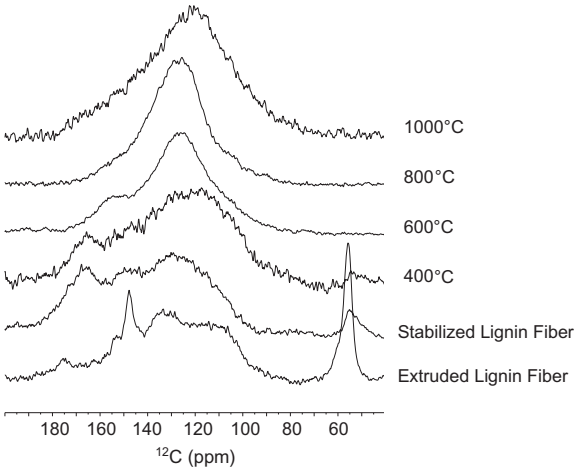

Fig. 7 – ^{13}C DP/MAS spectra of lignin and carbon fiber with a MAS condition of 12 kHz.

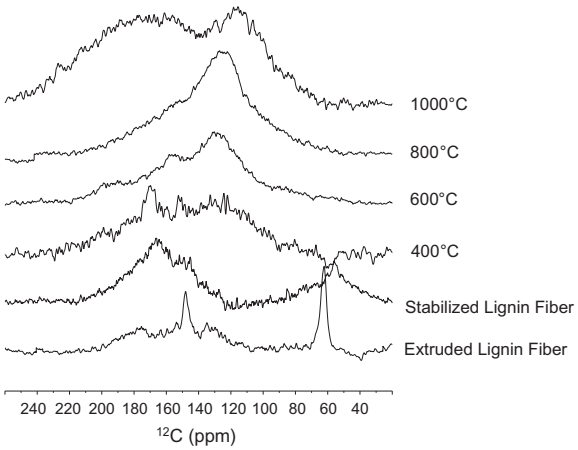

Fig. 8 – ^{13}C DP/MAS spectra of lignin and carbon fiber with a MAS condition of 12 kHz and 50 μs dipolar dephasing delay.

carbons. An important point to note is that the recycle delays for the DP experiments were set in an effort to obtain reasonable signal to noise and not necessarily generate quantitative spectra. Though true, the DP spectra provide additional information in conjunction with ^{1}H and ^{13}C CP experiments to determine possible changes occurring in the lignin fiber particularly during carbonization.

Further spectral analysis is provided by dipolar dephasing experiments, shown in Fig. 8, which suppresses the signals of rigid protonated carbons by introducing a 50 μs period of gated decoupling [35–38]. The resonances in Fig. 8 are due primarily either to carbonyl, quaternary aromatic or highly mobile methoxy carbons. After stabilization the majority of the peak intensity in Fig. 8 is attributed to resonances for carbonyl and methoxy groups. However, after carbonization at 400 °C, the methoxy resonance completely disappears, and the proportion of quaternary aromatic carbons increases. Again, this trend seems to continue with increasing carbonization temperature, shifting relative spectral resonance intensity to aromatic carbons near 123 ppm. Interestingly, the spectrum of the carbon fiber carbonized at 1000 °C does not display the same relatively narrow peak component at ~123 ppm, which had been progressively developing as the carbonization temperature was increased from 400 to 800 °C. This seems to suggest some sort of degradation is preferably affecting a portion of aryl structures at those high temperatures.

Solution ^{1}H–^{13}C HSQC experiments show that un-spun Alcell™ lignin is dominated by methoxy functionality, along with characteristic spectral signatures for β-aryl ether, phenyl coumaran and resinol linkages. Upon devolatilization/extrusion modest changes in the methoxylation and in the type and proportion of aliphatic side-chain carbons or monolignol inter-unit linkages occurred. GPC and ^{31}P NMR suggest fiber devolatilization/extrusion cause chain scission more than likely due to degradation in aliphatic side-chains and chain condensation reactions. These changes may be reflected in changes in macromolecular properties, suggesting manipulating devolatilization/extrusion conditions may provide critical control over macroscopic properties such as rheology and fiber orientational limits.

4. Conclusions

As part of this study, experiments have proven that NMR analysis can be applied to elucidate the mechanism(s) by which lignin is converted into carbon fiber. These techniques can be utilized to improve fiber processing conditions and understand how the resulting structures in the carbon fiber may enhance the mechanical properties of lignin-based composites. For example, rapid extrusion and oxidative stabilization of lignin-based carbon fiber precursor can lead to higher throughput and significant cost reduction in manufacturing. Therefore, understanding how time and temperature profiles affect the observed conversion mechanism will be critical to commercialization.

NMR techniques indicate that oxidative thermo-stabilization of Alcell™ lignin fiber causes: (1) some degradation or conversion of the most typical forms of lignin inter-unit linkages or aliphatic side-chain functionality, (2) demethoxylation and (3) the formation of carbonyl and carboxyl structures eventually displaying the increased presence of ester and anhydride functionality presumably due to cross-links within the oxidized lignin macromolecule. The application of other NMR methods suggest fiber carbonization leads to: (1) further reduction in the remaining methoxy content, (2) decreases in the relative amount of carbonyl and carboxyl structures, and (3) significant increases in the proportion of to aryl and condensed aryl carbons presumably as a result of fiber pyrolysis designed to drive off non-carbon atoms. Lastly these experiments indicate as carbonization temperature is increased the propensity to drive off oxygen containing functionality is greater, displaying a shifting relative spectral resonance intensity to aromatic carbons ~123 ppm. However, above 800 °C that trend reverses as spectral resonance intensity shift back towards ~150 ppm suggesting some sort of degradation is preferably affecting a portion of aryl structures at those high temperatures.

Acknowledgements

This work was supported and performed as part of research sponsored by the U.S. Department of Energy, Office of Energy Efficiency and Renewable Energy, Advanced Manufacturing Office, under contract DE-AC05-00OR22725 with UT-Battelle, LLC and the BioEnergy Science Center. The BioEnergy Science Center is a US Department of Energy Bioenergy Research Center supported by the Office of Biological and Environmental Research in the DOE Office of Science. ORNL is managed by UT-Battelle, LLC, under contract DE-AC05-00OR22725 for the US Department of Energy.

REFERENCES

[1] Kadla JF, Kubo S, Venditti RA, Gilbert RD, Compere AL, Griffith W. Lignin-based carbon fibers for composite fiber applications. Carbon 2002;40:2913–20.
[2] Riggs J. Gastric emptying of a nutritionally balanced liquid diet. In: Mark HF, Kroschwitz JI, editors. Encyclopedia of polymer science and engineering. New York: Wiley; 1985. p. 17.
[3] Donnet JB, Bahl OP. Encyclopedia of physical science and technology. New York: Academic Press; 1987.
[4] Chand S. Review carbon fibers for composites. J Mater Sci 2000;36:1303–13.
[5] Chung DL. Carbon fiber composites. New York: Butterworth–Heinemann; 1994. p. 13.
[6] Braun JL, Holtman KM, Kadla JF. Lignin-based carbon fibers: oxidative thermostabilization of kraft lignin. Carbon 2005;43:385–94.
[7] Gellerstedt G, Sjoholm E, Brodin I. The wood-based biorefinery: a source of carbon fiber? Open Agric J 2010;3:119–24.
[8] Shen Q, Zhang T, Zhang W, Chen S, Mezgebe M. Lignin-based activated carbon fibers and controllable pore size and properties. J Appl Polym Sci 2011;121:989–94.
[9] Atalla RH. Cellulose. In: Barton D, Nakanishi K, Meth-Cohn O, editors. Comprehensive natural products chemistry. Amsterdam, Netherlands: Elsevier; 1999.
[10] Fengel D, Wegener G. Wood: chemistry, ultrastructure, reactions. Berlin: W. de Gruyter; 1984. p. 132.
[11] Glasser WG, Kelley SS. Concise encyclopedia of polymer science and engineering. New York: Wiley; 1990. 544.

[12] Lora JH, Wu CF, Pye EK, Balatinecz JJ. Characteristics and potential applications of lignin produced by an organosolv pulping process. In: Glasser WG, Sarkanen S, editors. Lignin: properties and materials. American Chemical Society; 1989.
[13] Pu Y, Zhang D, Singh PM, Ragauskas AJ. The new forestry biofuels sector. Biofuels Bioprod Biorefin 2008;2:58–73.
[14] Ragauskas AJ, Williams CK, Davison BH, Britovsek G, et al. The path forward for biofuels and biomaterials. Science 2006;311(5760):484–9.
[15] Wazir AH, Kakakhel L. Preparation and characterization of pitch-based carbon fibers. New Carbon Mater 2009;24:83–8.
[16] Xiaojun M, Guangjie Z. Preparation of carbon fibers from liquefied wood. Wood Sci Technol 2010;44:3–11.
[17] Kubo S, Yoshida T. Surface porosity of lignin/PP blend carbon fibers. J Wood Chem Technol 2007;27:257–71.
[18] Bradley RH, Ling X, Sutherland I. An investigation of carbon fibre surface chemistry and reactivity based on XPS and surface free energy. Carbon 1993;31:1115–20.
[19] Shin S, Jang J, Yoon SH, Mochida I. A study on the effect of heat treatment on functional groups of pitch based activated carbon fiber using FTIR. Carbon 1997;35:1739–43.
[20] Baker D, Gallego N, Baker F. On the characterization and spinning of an organic-purified lignin toward the manufacture of low-cost carbon fiber. J Appl Polym Sci 2012;124:227–34.
[21] Jiang N, Pu Y, Samuel R, Ragauskas AJ. Perdeuterated pyridinium molten salt (ionic liquid) for direct dissolution and NMR analysis of plant cell walls. Green Chem 2009;11:1756–62.
[22] Pu Y, Cao S, Ragauskas AJ. Application of quantitative ^{31}P NMR in biomass lignin and biofuel precursors characterization. Energy Environ Sci 2011;4:3154–66.
[23] Pu Y, Anderson L, Lucia L, Ragauskas AJ. Fundamentals of photobleaching lignin. part 1: photobehaviors of acetylated softwood BCTMP lignin. J Pulp Paper Sci 2003;29:401.
[24] Samuel R, Foston M, Jaing N, Cao S, Ragauskas AJ, et al. HSQC (heteronuclear single quantum coherence) ^{13}C–^{1}H correlation spectra of whole biomass in perdeuterated pyridinium chloride–DMSO system: an effective tool for evaluating pretreatment. Fuel 2011;90:2836–42.
[25] Kim H, Ralph J. Solution-state 2D NMR of ball-milled plant cell wall gels in DMSO-d_6/pyridine-d_5. Org Chem Biomol Chem 2010;8:576–91.
[26] Zhang L, Gellerstedt G. Quantitative 2D HSQC NMR determination of polymer structures by selecting suitable internal standard references. Magn Reson Chem 2007;47:37–45.
[27] Granata A, Argyropoulos DS. 2-Chloro-4,4,5,5-tetramethyl-1,3,2-dioxaphospholane a reagent for the accurate determination of the uncondensed and condensed phenolic moieties in lignins. J Agric Food Chem 1995;46:1538–44.
[28] Lambert A. Review of gel permeation chromatography. Br Polym J 1971;3:13–23.
[29] Uraki Y, Kubo S, Nigo N, Sano Y, Sasaya T. Preparation of cabon fibers from organosolv lignin obtained by aqueous acetic acid pulping. Holzforschung 1995;49:343–50.
[30] Duer M. Introduction to solid-state NMR spectroscopy. Oxford: Blackwell; 2004.
[31] Lundquist K. NMR stduies of lignins 4. Investigation of spruce lignin by ^{1}H NMR spectroscopy. Acta Chem Scand B 1980;34:21–6.
[32] Gil AM, Lopes MH, Neto CP, Rocha J. Very high-resolution ^{1}H MAS NMR of a natural polymeric material. Solid State Nucl Magn Reson 1999;15:56–67.
[33] Bardet M, Foray MF, Guillermo A. High-resolution solid-state NMR as an analytical tool to study plant seeds. In: Webb GA, editor. Modern magnetic resonance. New York: Springer; 2006.
[34] Bardet M, Foray MF, Tran QK. High-resolution solid-state CPMAS NMR study of archaeological woods. Anal Chem 2002;74:4386–90.
[35] Hatcher P. Chemical structural studies of natural lignin by dipolar dephasing solid-state ^{13}C nuclear magnetic resonance. Org Geochem 1987;11:31–9.
[36] Mao JD, Schmidt-Rohr K. Accurate quantification of aromaticity and nonprotonated aromatic carbon fraction in natural organic matter by ^{13}C solid-state nuclear magnetic resonance. Environ Sci Technol 2004;38:2680–4.
[37] Mao J, Holtman KM, Scott JT, Kadla J, Schmidt-Rohr K. Differences between lignin in unprocessed wood, milled wood, mutant wood, and extracted lignin detected by ^{13}C Solid-State NMR. J Agric Food Chem 2006;54:9677–86.
[38] Liitia T, Maunu SL, Sipila J, Hortling B. Application of solid-state ^{13}C NMR spectroscopy and dipolar dephasing technique to determine the extent of condensation in technical lignins. Solid State Nucl Magn Reson 2002;21:171–86.